Published in final edited form as:

Cell Metab. 2017 November 07; 26(5): 709–718.e3. doi:10.1016/j.cmet.2017.09.005.

FGF19, FGF21 and an FGFR1/β-Klotho-activating Antibody Act on the Nervous System to Regulate Body Weight and Glycemia

Tian Lan[1,2], **Donald A. Morgan**[6], **Kamal Rahmouni**[6], **Junichiro Sonoda**[7], **Xiaorong Fu**[3], **Shawn C. Burgess**[1,3], **William L. Holland**[4], **Steven A. Kliewer**[1,2,8,*], and **David J. Mangelsdorf**[1,5,8,9,*]

[1]Department of Pharmacology, UT Southwestern Medical Center, Dallas, TX 75390 USA

[2]Department of Molecular Biology, UT Southwestern Medical Center, Dallas, TX 75390 USA

[3]Center for Human Nutrition, UT Southwestern Medical Center, Dallas, TX 75390 USA

[4]Touchstone Diabetes Center, Department of Internal Medicine, UT Southwestern Medical Center, Dallas, TX 75390 USA

[5]Howard Hughes Medical Institute, UT Southwestern Medical Center, Dallas, TX 75390 USA

[6]Department of Pharmacology, University of Iowa Carver College of Medicine, Iowa City, IA 52242 USA

[7]Molecular Biology, Genentech Inc., South San Francisco, CA 94080 USA

Abstract

Despite their different physiologic functions as hormonal regulators of fed and fasted metabolism, pharmacologic administration of FGF19 and FGF21 similarly cause increases in energy expenditure, weight loss and enhanced insulin sensitivity in obese animals. Here, in genetic loss-of-function studies of the shared co-receptor β-Klotho, we show these pharmacologic effects are mediated through a common tissue-specific pathway. Surprisingly, FGF19 and FGF21 actions in liver and adipose tissue are not required for their longer-term weight loss and glycemic effects. In contrast, β-Klotho in neurons is essential for both FGF19 and FGF21 to cause weight loss and lower glucose and insulin levels. We further show that an FGF21 mimetic antibody that activates the FGF receptor 1/β-Klotho complex also requires neuronal β-Klotho for its metabolic effects. These studies highlight the importance of the nervous system in mediating the beneficial weight loss and glycemic effects of endocrine FGF drugs.

[*]Correspondence: steven.kliewer@utsouthwestern.edu (S.A.K.), davo.mango@utsouthwestern.edu (D.J.M.).
[8]Senior authors
[9]Lead contact

Author Contributions

T.L. designed, performed, and analyzed experiments and wrote the paper; D.A.M. and K.R. performed and analyzed sympathetic nerve activity experiments; J.S. designed experiments and provided the bFKB1 antibody; X.F. and S.C.B. performed amino acid and acylcarnitine measurements; W.L.H. designed and analyzed experiments; S.A.K. and D.J.M. supervised the project, designed and analyzed experiments, and wrote the paper. All authors commented on and approved the paper.

eTOC

The tissue-specific actions of FGF19- and FGF21-based therapeutics have stimulated considerable scientific and clinical interest. Lan et al. show that FGF19, FGF21 and an antibody mimetic require the co-receptor, β-Klotho, in neurons, but not hepatocytes or adipocytes, to mediate their beneficial metabolic effects on body weight and glycemia.

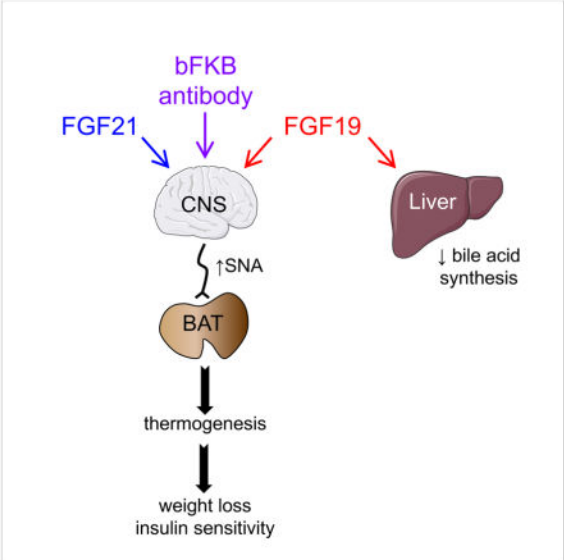

Introduction

Fibroblast growth factors (FGFs) 19 and 21 are members of an atypical subfamily of FGFs that can circulate as hormones (Fisher and Maratos-Flier, 2016; Kharitonenkov and DiMarchi, 2017; Owen et al., 2015). FGF19 is induced by postprandial bile acids in small intestine and represses bile acid synthesis and induces glycogen and protein synthesis in the liver. FGF21 is induced by starvation and low protein, ketogenic and high carbohydrate diets in liver and has broad effects on glucose and fatty acid metabolism. Although FGF19 and FGF21 have different physiologic functions, paradoxically they have similar pharmacologic effects. Both increase energy expenditure and decrease body weight, blood glucose and insulin, and hepatic triglyceride concentrations in rodent models of obesity (Coskun et al., 2008; Fu et al., 2004; Kharitonenkov et al., 2005; Tomlinson et al., 2002; Xu et al., 2009).

FGF19 and FGF21 act through cell surface receptors comprised of conventional FGF receptors (FGFRs) with tyrosine kinase activity in complex with the single-pass transmembrane protein β-Klotho (Kuro-o, 2012). Both FGF19 and FGF21 act on β-Klotho in complex with FGFR1c, 2c and 3c. FGFRs 1, 2 and 3 and β-Klotho are relatively abundantly expressed in brown adipose tissue (BAT), white adipose tissue (WAT) and regions in the nervous system, including the hypothalamus and hindbrain (Bookout et al., 2013; Fon Tacer et al., 2010). FGF19, but not FGF21, also activates the FGFR4/β-Klotho heteromer, which is abundantly expressed in liver, where it is required for FGF19 to mediate its effects on bile acid and glycogen synthesis (Fon Tacer et al., 2010; Ito et al., 2005;

Katafuchi et al., 2015; Yu et al., 2000). Interestingly, monoclonal antibodies that selectively activate either FGFR1 (Wu et al., 2011b) or the FGFR1/β-Klotho heteromer (Foltz et al., 2012; Kolumam et al., 2015) recapitulate the effects of FGF19 and FGF21 on body weight and circulating glucose and insulin concentrations in obese rodents and monkeys, suggesting that the FGFR1/β-Klotho heteromer is a key target for the pharmacologic actions of these endocrine FGFs.

Given their striking pharmacologic profiles, there is intense interest in understanding how FGF19 and FGF21 regulate metabolism. FGF21 stimulates energy expenditure in part by acting directly on the nervous system to induce sympathetic outflow to BAT and white adipose tissue (WAT) (Douris et al., 2015; Owen et al., 2014). Similarly, intracerebroventricular (i.c.v.) injection of FGF19 directly into the brain increases metabolic rate and decreases circulating glucose and insulin concentrations (Fu et al., 2004; Marcelin et al., 2014; Morton et al., 2013; Ryan et al., 2013). FGF21 also acts directly on adipocytes to stimulate glucose uptake, thermogenic gene expression and adiponectin secretion (Fisher et al., 2012; Holland et al., 2013; Hondares et al., 2010; Kharitonenkov et al., 2005; Lin et al., 2013). Accordingly, the anti-obesity and anti-diabetic effects of FGF21 – but not FGF19 – were either absent or attenuated in obese mice in which the *Fgfr1* gene was disrupted in adipose and other tissues using a non-selective *aP2*-Cre driver (Adams et al., 2012; Foltz et al., 2012). These data and the finding that high molecular weight FGF21 derivatives, which presumably cannot penetrate the brain, retain their metabolic actions, led to the hypothesis that adipose is the principal FGF21 target tissue (Kharitonenkov and Adams, 2014). Finally, both FGF19 and FGF21 act on liver to regulate metabolism (Fisher et al., 2011; Kir et al., 2011). However, the relative importance of nervous system, adipose tissue and liver in mediating the long-term metabolic actions of FGF19, FGF21 and their mimetic antibodies remains unclear.

In this report we use mice selectively lacking β-Klotho in hepatocytes, adipocytes or neurons to systematically compare the tissue-specific mechanisms underlying the pharmacologic actions of FGF19, FGF21 and the humanized, bispecific FGFR1/β-Klotho-activating antibody, bFKB1 (Kolumam et al., 2015). Surprisingly, we find that all three molecules require β-Klotho in neurons, but not hepatocytes or adipocytes, to mediate their chronic metabolic effects on body weight and glycemia.

Results

β-Klotho in hepatocytes is not required for FGF19 and FGF21 to cause weight loss

Since hepatocytes express abundant levels of β-Klotho and are known to respond to FGF19 and FGF21, we first characterized the metabolic phenotype of mice lacking β-Klotho specifically in hepatocytes (Klb^{Alb} mice). In agreement with our previous results (Katafuchi et al., 2015), Klb^{Alb} mice had increased hepatic expression of cholesterol 7α-hydroxylase (*Cyp7a1*), which encodes the rate-limiting enzyme in bile acid synthesis (Figure 1A and S1A). We have shown this increase in *Cyp7a1* expression is due to the loss of feedback regulation of *Cyp7a1* by FGF15, the mouse ortholog of FGF19, and occurs despite a marked compensatory increase in FGF15 protein in plasma (Katafuchi et al., 2015). Thus, FGF15/β-Klotho signaling in liver is required for the physiologic regulation of bile acid homeostasis.

To examine whether the elevated levels of FGF15 in *Klb*^{Alb} mice might also affect body weight and other metabolic parameters, groups of control floxed β-Klotho (*Klb*$^{fl/fl}$) mice and *Klb*^{Alb} mice were fed a high fat diet. As expected, diet-induced obese (DIO) *Klb*^{Alb} mice had increases in both *Fgf15* mRNA levels in ileum and FGF15 concentrations in plasma (Figure S1B). Despite a marked 10-fold increase in plasma FGF15 levels, *Klb*^{Alb} mice were indistinguishable from *Klb*$^{fl/fl}$ littermates with respect to body weight and body composition after 7 weeks on the high fat diet (Figure S1C). Under hyperinsulinemic-euglycemic clamp conditions, there was no difference between DIO *Klb*$^{fl/fl}$ and *Klb*^{Alb} mice in glucose infusion rate, endogenous glucose production, whole body glucose uptake or basal endogenous glucose production (Figure S1D). In metabolic cage studies, there were no differences between DIO *Klb*$^{fl/fl}$ and *Klb*^{Alb} mice in food consumption, locomotor activity and heat production (Figure S1E). Thus, we see no evidence that endogenous FGF15, even at levels as high as 20 ng/ml, has direct metabolic effects on tissues other than liver.

We next compared the acute effects of FGF19 and FGF21 administration on liver in DIO *Klb*$^{fl/fl}$ and *Klb*^{Alb} mice. FGF19 treatment increased hepatic ERK1/2 phosphorylation and *Egr1* expression and dramatically decreased *Cyp7a1* expression in control *Klb*$^{fl/fl}$ but not *Klb*^{Alb} mice (Figures 1A–C). In contrast, FGF21 treatment did not affect ERK1/2 phosphorylation or *Egr1* expression and caused only a downward trend in *Cyp7a1* mRNA levels in *Klb*$^{fl/fl}$ mice (Figures 1A–C). The weak effect of acute FGF21 administration on *Cyp7a1* expression is consistent with previous studies (Wu et al., 2011a; Zhang et al., 2017). We conclude that FGF19, but not FGF21, has robust, direct effects on hepatocytes under acute pharmacologic treatment conditions.

To determine whether FGF19 and FGF21 mediate their longer-term metabolic effects by acting directly on hepatocytes, groups of DIO *Klb*$^{fl/fl}$ and *Klb*^{Alb} mice were administered FGF19, FGF21 or vehicle for 2 weeks. While FGF21 was delivered by osmotic minipump, FGF19 was administered by once-daily subcutaneous injection because it precipitated in the minipumps. As expected, both FGF19 and FGF21 decreased body weight, plasma glucose and hepatic triglyceride levels in DIO *Klb*$^{fl/fl}$ mice (Figures 2A and B). Notably, FGF19 and FGF21 elicited these same effects in *Klb*^{Alb} mice (Figures 2A and B), demonstrating that these metabolic actions do not require FGF19 and FGF21 to act directly on liver. FGF19 and FGF21 did not significantly affect hepatic cholesterol concentrations in *Klb*$^{fl/fl}$ or *Klb*^{Alb} mice (Figure 2B). Whereas FGF21 modestly increased adiponectin levels in both *Klb*$^{fl/fl}$ and *Klb*^{Alb} mice, FGF19 did not have these effects in either genotype (Figure 2B).

In gene expression studies, FGF19 increased mRNA expression of dual specificity phosphatase 4 (*Dusp4*), which is involved in the feedback regulation of ERK1/2, in liver in *Klb*$^{fl/fl}$ but not *Klb*^{Alb} mice (Figure S2A). In contrast, FGF21 did not increase hepatic *Dusp4* expression in either genotype (Figure S2A). Both FGF19 and FGF21 decreased hepatic lipogenic gene expression (*Fas*, *Scd1*) in *Klb*$^{fl/fl}$ and *Klb*^{Alb} mice (Figure S2A), demonstrating that these effects do not require the FGFs to act directly on hepatocytes. In BAT, both FGF19 and FGF21 increased expression of *Dusp4* and the thermogenic genes deiodinase 2 (*Dio2*), bone morphogenic protein 8b (*Bmp8b*) and elongation of very long chain fatty acids 3 (*Elovl3*) in *Klb*$^{fl/fl}$ and *Klb*^{Alb} mice (Figure S2B). Thus, these effects do not require FGF19 or FGF21 to act on hepatocytes. Neither FGF19 nor FGF21 affected

Ucp1 expression in BAT or scWAT under these treatment conditions (Figures S2B and C). Taken together these experiments demonstrate that the majority of the metabolic effects of FGF19 and FGF21, including those on weight loss and glycemia, are not mediated through direct actions on liver.

β-Klotho in adipose tissue is required for the acute insulin-sensitizing actions of FGF19 and FGF21

We previously showed that the acute insulin-sensitizing effect of FGF21 was lost in DIO mice in which β-Klotho was eliminated in adipose tissue using the *aP2*-Cre driver (Ding et al., 2012). However, these Klb^{aP2} mice also had decreased *Klb* expression in the nervous system, where the *aP2* promoter is active (Ding et al., 2012; Martens et al., 2010). To avoid this confounding issue, we generated knockout mice using the adiponectin (*Adipoq*)-Cre driver, which disrupted *Klb* expression in both BAT and subcutaneous (sc) WAT but not in liver or hypothalamus (Figure S1A).

Hyperinsulinemic-euglycemic clamp experiments were performed in DIO $Klb^{fl/fl}$ and Klb^{Adipoq} mice treated acutely with FGF19 or FGF21. Consistent with our previous findings (Ding et al., 2012), FGF21 administration increased glucose infusion rate and whole-body glucose uptake in $Klb^{fl/fl}$ but not Klb^{Adipoq} mice (Figure 3A). FGF21 also suppressed endogenous glucose production in $Klb^{fl/fl}$ but not Klb^{Adipoq} mice under clamp conditions (Figure 3A). Like FGF21, FGF19 treatment significantly increased the glucose infusion rate and whole-body glucose uptake in $Klb^{fl/fl}$ but not Klb^{Adipoq} mice (Figure 3B). However, unlike FGF21, FGF19 caused a downward trend in endogenous glucose production in both $Klb^{fl/fl}$ and Klb^{Adipoq} mice (Figure 3B), suggesting that FGF19 may be acting on other, non-adipose tissues such as liver (Kir et al., 2011). Taken together, the clamp data show that under acute treatment conditions, both FGF19 and FGF21 act directly on adipose tissue to increase whole-body insulin sensitivity.

β-Klotho in adipose tissue is not required for FGF19 and FGF21 to cause weight loss

To determine whether FGF19 and FGF21 mediate their longer-term metabolic effects by acting directly on adipose tissue, groups of DIO $Klb^{fl/fl}$ and Klb^{Adipoq} mice were administered FGF19, FGF21 or vehicle for 2 weeks. Both FGF19 and FGF21 decreased body weight, plasma insulin and glucose concentrations, and hepatic triglyceride concentrations in control $Klb^{fl/fl}$ and Klb^{Adipoq} mice (Figures 4A and B). FGF21 modestly increased plasma adiponectin levels in $Klb^{fl/fl}$ but not Klb^{Adipoq} mice (Figure 4B), consistent with previous studies showing that FGF21 acts directly on adipocytes to stimulate adiponectin secretion (Holland et al., 2013; Lin et al., 2013). However, hepatic concentrations of ceramides, which can be reduced by adiponectin, were unchanged by FGF21 in $Klb^{fl/fl}$ and Klb^{Adipoq} mice (Figure 4B). FGF19 caused modest decreases in plasma adiponectin levels in both $Klb^{fl/fl}$ and Klb^{Adipoq} mice with no significant changes in hepatic ceramide levels (Figure 4A). We also analyzed hepatic diacylglycerol (DAG) and plasma acylcarnitine and branched-chain amino acid (BCAA) concentrations. Hepatic DAG concentrations were significantly reduced by FGF19 in Klb^{Adipoq} mice with a similar downward trend in $Klb^{fl/fl}$ mice (Figure S3D). FGF21 administration did not significantly affect DAG levels in either $Klb^{fl/fl}$ or Klb^{Adipoq} mice (Figure S3D). Plasma acylcarnitine

concentrations were unchanged by FGF19 or FGF21 in $Klb^{fl/fl}$ and Klb^{Adipoq} mice (Figure S3E). Plasma valine concentrations were modestly increased in response to FGF21 in $Klb^{fl/fl}$ mice and trended upward in Klb^{Adipoq} mice but were unchanged by FGF19 treatment in either genotype (Figure S3F). Plasma leucine and isoleucine concentrations were unchanged by either FGF19 or FGF21 in $Klb^{fl/fl}$ and Klb^{Adipoq} mice (Figure S3F). We conclude that the longer-term weight loss and glycemic effects of FGF19 and FGF21 in this DIO model do not require that they act directly on adipose tissue, and that there is no clear correlation between FGF19 and FGF21 action and hepatic ceramide and DAG concentrations or plasma acylcarnitine and BCAA concentrations.

In gene expression studies, FGF19 and FGF21 induced *Dusp4* mRNA in BAT and scWAT in $Klb^{fl/fl}$ but not Klb^{Adipoq} mice, demonstrating that the FGFs act directly on adipocytes (Figures S3A and B). In contrast, *Dio2*, *Bmp8b* and *Elovl3* were induced in BAT by FGF19 and FGF21 in both $Klb^{fl/fl}$ and Klb^{Adipoq} mice (Figure S3A). While these data reveal that FGF19 and FGF21 have both direct and indirect effects on adipose tissue, the chronic metabolic actions of these FGFs do not require that they act directly on adipocytes.

FGF19 acts on the nervous system to cause weight loss

The ability of FGF19 to cause weight loss and lower plasma glucose and insulin levels in the DIO Klb^{Adipoq} knockout model led us to examine whether FGF19, like FGF21, acts via the nervous system. To test this, groups of DIO $Klb^{fl/fl}$ and Klb^{Camk2a} mice, in which β-Klotho expression was selectively disrupted in the nervous system (Figure S1A), were administered vehicle or FGF19 for 2 weeks. FGF19 caused weight loss in $Klb^{fl/fl}$ mice, which was accompanied by decreases in plasma glucose and hepatic triglyceride concentrations and a downward trend in plasma insulin levels (Figure 5A). In contrast, FGF19 had no effect on these parameters in Klb^{Camk2a} mice (Figure 5A). We conclude that FGF19, like FGF21, acts on the nervous system to mediate its longer-term effects on body weight, circulating glucose and insulin concentrations, and liver triglyceride levels.

In gene expression analyses, FGF19 induced *Dusp4* in BAT, scWAT and liver in both $Klb^{fl/fl}$ and Klb^{Camk2a} mice (Figure S4), demonstrating that FGF19 acts directly on each of these tissues. In BAT, FGF19 increased *Dio2*, *Bmp8b* and *Elovl3* expression in $Klb^{fl/fl}$ but not Klb^{Camk2a} mice (Figure S4), demonstrating that induction of these genes requires FGF19 to act on the nervous system.

We next tested whether FGF19 induces sympathetic outflow to BAT and increases energy expenditure, as we observed with FGF21 (Owen et al., 2014). Sympathetic nerve activity was measured directly in interscapular BAT in mice administered FGF19 or vehicle by either i.c.v. or peripheral intravenous (i.v.) injection. Under both treatment conditions, FGF19 induced sympathetic nerve activity 1.5–2 hr after injection in a dose-dependent manner (Figure 5B). FGF19 administration caused a corresponding increase in energy expenditure that was present in both the light and dark phases of the daily light cycle (Figure 5C). FGF19 treatment did not change food intake or locomotor activity in these mice (Figure 5D). Thus, like FGF21, FGF19 stimulates sympathetic outflow to BAT and causes corresponding increases in energy expenditure.

An FGFR1/β-Klotho activating antibody acts on neurons to cause weight loss

Antibodies that selectively activate either FGFR1 or the FGFR1/β-Klotho heteromer recapitulate many of the metabolic actions of FGF19 and FGF21, including their effects on body weight and glucose and insulin concentrations in obese mice (Foltz et al., 2012; Kolumam et al., 2015; Wu et al., 2011b). However, given their high molecular weights, it was unclear whether these antibodies permeate the brain or act in the nervous system like FGF19 and FGF21. We first tested the FGFR1/β-Klotho bispecific antibody (bFKB1) (Kolumam et al., 2015) in the adipose tissue-specific β-Klotho knockout model. Groups of DIO $Klb^{fl/fl}$ and Klb^{Adipoq} mice were treated with bFKB1 or control antibody (trastuzumab, which does not bind to mouse HER2 and has no known activity in mice) for 4 weeks. bFKB1 administration caused weight loss in both groups (Figure 6A). bFKB1 also decreased plasma glucose and hepatic triglyceride levels in both $Klb^{fl/fl}$ and Klb^{Adipoq} mice (Figure 6A). bFKB1 did not significantly increase plasma adiponectin concentrations in either genotype (Figure 6A). Thus, bFKB1 exerts its effects on body weight and other metabolic parameters without acting directly on adipocytes.

In gene expression studies, bFKB1 induced *Dusp4* in BAT in $Klb^{fl/fl}$ but not Klb^{Adipoq} mice (Figure S5A), demonstrating that bFKB1 acts directly on BAT. bFKB1 increased *Ucp1*, *Dio2*, *Bmp8b* and *Elovl3* expression in BAT in both $Klb^{fl/fl}$ and Klb^{Adipoq} mice (Figure S5A), demonstrating that these effects do not require the antibody to act directly on adipocytes. In liver, bFKB1 decreased *Dusp4* and *Scd1* expression in both $Klb^{fl/fl}$ and Klb^{Adipoq} mice, demonstrating that these effects are independent of direct effects on adipocytes (Figure S5A).

We next tested bFKB1 in the neuron-specific β-Klotho knockout model. Notably, bFKB1 decreased body weight and plasma glucose concentrations in control $Klb^{fl/fl}$ mice but not Klb^{Camk2a} knockout mice (Figure 6B). A similar trend was seen with plasma insulin and hepatic triglyceride levels (Figure 6B). Thus, these metabolic actions of bFKB1 require β-Klotho in the nervous system. bFKB1 did not significantly increase plasma adiponectin concentrations in either genotype (Figure 6B). In gene expression analyses, bFKB1 induced *Dusp4* in BAT in both $Klb^{fl/fl}$ and Klb^{Camk2a} mice (Figure S5B). In contrast, bFKB1 induced *Bmp8b* and *Elovl3* in BAT of $Klb^{fl/fl}$ but not Klb^{Camk2a} mice (Figure S5B). The induction profile of these genes mirrors the weight loss and glycemia data in the Klb^{Camk2a} knockout model.

The Klb^{Camk2a} knockout studies demonstrate that bFKB1 acts on neurons to affect body weight and circulating glucose and insulin levels despite its high molecular weight. To test whether bFKB1 crosses the blood-brain barrier, we measured bFKB1 concentrations in cerebrospinal fluid (CSF) and plasma 2 weeks after bFKB1 injection. The concentrations of bFKB1 in the CSF and plasma were 0.15 μg/ml and 150 μg/ml, respectively (Figure 6C). Although the bFKB1 CSF:plasma ratio was low, this bFKB1 concentration (~1 nM) in the CSF is sufficient to activate the FGFR1/β-Klotho receptor based on previous studies (Kolumam et al., 2015).

Discussion

How FGF19 and FGF21 mediate their potent pharmacologic effects is a key question in the endocrine FGF field, especially since clinical trials are underway with long-acting analogs of both. Here, we show that both FGF19 and FGF21, as well as the bFKB1 antibody, require their receptor complex in neurons, but not hepatocytes or adipocytes, to cause weight loss and reduce circulating glucose and insulin concentrations. Moreover, FGF19, like FGF21, stimulates sympathetic outflow to BAT. While we did not directly measure the effect of bFKB1 on sympathetic outflow, the antibody induced the expression of genes regulated by the β-adrenergic receptor pathway, including *Bmp8b* and *Elovl3*, in BAT of $Klb^{fl/fl}$ but not Klb^{Camk2a} mice. This gene expression profile, which mirrors those of FGF19 and FGF21, is consistent with bFKB1 also stimulating sympathetic nervous system activity. Taken together, these data show that all three molecules act through a similar if not identical neuron-mediated mechanism.

In two previous studies, the effects of FGF19 (Adams et al., 2012) or FGF21 (Adams et al., 2012; Foltz et al., 2012) were examined in DIO mice in which the *Fgfr1* gene was disrupted in adipose tissue using an *aP2*-Cre driver. In these knockout mice, the effects of FGF21 on body weight and circulating glucose and insulin were either absent or attenuated (Adams et al., 2012; Foltz et al., 2012). In contrast, the effects of FGF19 on these parameters were unaffected in the knockout mice (Adams et al., 2012). Based on these data, it was suggested that FGF19 and FGF21 act principally through liver and adipose tissue, respectively. However, the *aP2*-Cre driver is also active in the nervous system (Martens et al., 2010), where we showed that it efficiently reduced *Klb* expression when crossed into the $Klb^{fl/fl}$ mice (Ding et al., 2012). Given that the metabolic effects of FGF21 still occur in the Klb^{Adipoq} mice, we suggest that these previous findings were primarily a consequence of disrupted *Fgfr1* expression in nervous system. Regarding FGF19, it is possible that it acts through an FGFR other than FGFR1c in neurons. However, our data show that both FGF19 and FGF21 act through the nervous system and activate sympathetic outflow to BAT, indicating a similar mechanism of action. Others have shown that FGF19 suppresses the HPA axis (Perry et al., 2015) and AGRP/NPY neuronal activity (Marcelin et al., 2014). Thus, FGF19 and FGF21 likely exert their metabolic effects via multiple pathways in the nervous system.

Do FGF19, FGF21 and bFKB1 work inside the blood-brain barrier? Both FGF19 and FGF21 cross the blood-brain barrier at pharmacologic doses (Hsuchou et al., 2007, 2013), and direct i.c.v. injection of FGF19 or FGF21 into the brain stimulates energy expenditure and reduces glycemia (Marcelin et al., 2014; Morton et al., 2013; Perry et al., 2015; Ryan et al., 2013; Sarruf et al., 2010). Moreover, β-Klotho and FGFRs are expressed in the central nervous system (Bookout et al., 2013; Fon Tacer et al., 2010). These data suggest that FGF19 and FGF21 act centrally. While bFKB1 is much larger than FGF19 and FGF21, at least some antibodies are able to penetrate the blood-brain barrier, albeit inefficiently: CSF levels are approximately 1000-fold lower than in blood (Tabrizi et al., 2010). The level of bFKB1 that we detected in the CSF is consistent with these findings. Importantly, however, this concentration is above that required to activate the FGFR/β-Klotho receptor complex (Kolumam et al., 2015). These data together with our finding that the kinetics of weight loss

were slower with bFKB1 than either FGF19 or FGF21, suggest that bFKB1 may cross blood-brain barrier and accumulate to concentrations that are sufficient to activate FGFR/β-Klotho receptors in the central nervous system. Notably, our results do not rule out effects in neurons outside the blood-brain barrier. Regardless, the results clearly indicate that the nervous system, and not adipose tissue, is required for the weight loss effects of all three drugs.

FGF19 and FGF21 also act on peripheral tissues to regulate glucose metabolism. Here we show that under hyperinsulinemic-euglycemic clamp conditions, both FGF19 and FGF21 increase insulin sensitivity and stimulate whole-body glucose uptake by acting directly on adipose tissue. Our data agree with a recent study in which the acute insulin-sensitizing effect of FGF21 was absent in mice lacking β-Klotho in adipose tissue (BonDurant et al., 2017). Previous studies showed that FGF21 stimulates glucose uptake into BAT (Ding et al., 2012; Markan et al., 2014; Xu et al., 2009), which likely provides substrate for uncoupled oxidation and thermogenesis. FGF21 also acts on WAT to stimulate adiponectin secretion (Holland et al., 2013; Lin et al., 2013). However, our studies with Klb^{Adipoq} mice show that the longer-term effects of FGF19 and FGF21 on body weight and glycemia do not require that they act directly on adipocytes nor that they activate the adiponectin-ceramide axis. We note that the glycemic effects of FGF19 and FGF21 in this DIO model may be secondary to the weight loss.

A final key finding of our work is that the liver, which expresses abundant levels of β-Klotho, is not required for the long-term glycemic and weight loss effects of either FGF19 or FGF21. Previous work showed that FGF19 works directly on hepatocytes to govern postprandial bile acid metabolism and glycogen storage (Kir et al., 2011). Accordingly, Klb^{Alb} mice have increased hepatic bile acid synthesis and decreased hepatic glycogen levels despite a large compensatory increase in FGF15 concentrations in blood (Katafuchi et al., 2015). Our present studies demonstrate that this direct effect of FGF19 on hepatocytes to induce glycogen storage is not required for FGF19's longer-term effect on glycemia in the DIO model. Our data further show that there is little direct effect of FGF21 on hepatocytes, which is consistent with little or no expression of FGFR1c, the preferred tyrosine kinase receptor for FGF21, in hepatocytes (Fon Tacer et al., 2010). Thus, we conclude that the primary role of β-Klotho in the liver is to mediate the postprandial actions of FGF19.

In closing, we find that FGF19, FGF21 and bFKB1 all require β-Klotho-containing receptor complexes in neurons to decrease body weight and circulating glucose and insulin concentrations in the DIO mouse model. Moreover, FGF19 increases sympathetic outflow to BAT, just like FGF21. These findings suggest that the therapeutic efficacy of FGF19 and FGF21-based drugs, including activating antibodies, for treating metabolic disease will depend on their ability to access and activate the nervous system.

STAR METHODS

CONTACT FOR REAGENT AND RESOURCE SHARING

Further information and requests for resources and reagents should be directed to and will be fulfilled by the Lead Contacts, Steven Kliewer (steven.kliewer@utsouthwestern.edu) and David Mangelsdorf (davo.mango@utsouthwestern.edu).

EXPERIMENTAL MODEL AND SUBJECT DETAILS

All procedures and use of mice were approved by the Institutional Animal Care and Use Committee of University of Texas Southwestern Medical Center.

Generation of Klb^{Alb} mice was as described (Katafuchi et al., 2015). Generation of Klb^{Camk2a} mice was as described (Bookout et al., 2013). Klb^{Adipoq} mice were generated by breeding *Adipoq*-Cre mice (Jackson Laboratory) with $Klb^{fl/fl}$ mice (Bookout et al., 2013). Klb^{Adipoq} mice were on C57BL/6J background. Klb^{Alb} mice were on mixed C57BL/6J; 129/Sv background. Klb^{Camk2a} mice were on mixed C57BL/6J;129/Sv background.

C57BL/6J mice were generated from the animal breeding core at University of Texas Southwestern Medical Center.

Mice were maintained on a 12 hr light-dark cycle with lights on at 7 am. Housing rooms were maintained at 22–23°C. Mice were maintained on a rodent chow (Harlan Teklad, TD. 2916) until 3–4 months of age prior to initiating the experiments. Male mice and wild-type littermate controls were used in all experiments. Mice were randomly assigned to experimental groups based on body weight.

METHOD DETAILS

Mouse Studies—At 3–4 months of age, mice were switched from normal rodent chow to a high fat diet to cause obesity (Research Diets, D12492i). All groups of DIO mice had an average body weight >40 g/mouse at the start of experiments. Mice were randomly assigned to experimental groups based on body weight. Body composition was measured using an EchoMRI-100 body composition analyzer. Indirect calorimetry to measure energy expenditure was performed using LabMaster metabolic cages (TSE systems), with values normalized to lean body mass. Energy expenditure was calculated as a function of O_2 consumption and CO_2 production according to the following formula: EE (kcal/hr) = (3.941 x vO_2 (ml/hr) + 1.106 x vCO_2 (ml/hr))/1,000. Housing rooms were maintained at 22–23°C. Metabolic cage studies were performed at 21–22°C. All mice were sacrificed by decapitation.

FGF21, FGF19 and bFKB1 Administration—Recombinant human FGF21 was from Novo Nordisk (Malov, Denmark) and was stored in a buffer containing 10 mM Na_2HPO_4 and 2% (w/v) glycerol at pH 7.6. Recombinant human FGF19 was synthesized as described (Choi et al., 2006) and stored in a buffer containing 150 mM NaCl, 20 mM Tris and 50% (w/v) glycerol at pH 7.5. bFKB1 and trastuzumab were from Genentech (South San Francisco, CA).

For the acute ERK1/2 phosphorylation and *Egr1* induction studies (but not the hyperinsulinemic-euglycemic clamp or sympathetic nerve activity studies, which are described below), mice were fasted for 5 hr and intraperitoneally (i.p.) injected with a single bolus of FGF19 or FGF21 (1 mg/kg) or vehicle alone and sacrificed 30 min later. For studies of acute FGF19 and FGF21 effects on hepatic *Cyp7a1* expression, ad-lib fed mice were i.p. injected with 1 mg/kg FGF19, FGF21 or vehicle and sacrificed 6 hr later.

For chronic FGF21 treatment, osmotic pumps (Alzet Micro-Osmotic Pump Model 1002) were s.c. implanted under isofluorane inhalation anesthesia. FGF21 was delivered at a dose of 1 mg/kg/day. For chronic FGF19 treatment, mice were s.c. injected once daily with 1 mg/kg FGF19 or vehicle. For chronic bFKB1 treatment, mice were i.p. injected with 10 mg/kg bFKB1 or control antibody (trastuzumab) once every two weeks. Mice in chronic FGF19 and FGF21 experiments were sacrificed under ad lib fed conditions between 1–3 pm. Mice in chronic bFKB1 experiments were fasted for 4 hr and sacrificed between 1–3 pm.

Plasma and Liver Analyses—Blood was collected into EDTA-coated tubes (Sarstedt, Newton, NC). Plasma was separated by centrifugation and assayed for glucose (Wako Diagnostics), insulin (Crystal Chem), adiponectin (Millipore), total plasma cholesterol (Pointe Scientific) and triglyceride levels (Thermo Scientific). Plasma FGF15 protein levels were measured using the SISCAPA-SRM assay as described (Katafuchi et al., 2015). For plasma BCAA analysis, thawed plasma samples were immediately spiked with labeled amino acid internal standard (Isotec) and cold acetone. The extraction and derivatization of amino acids from plasma were performed as described (Casetta et al., 2000). Amino acids were separated on a reverse phase C18 column (Xbridge, Waters, Milford, MA; 150×2.1 mm, 3.0μm) with a gradient elution and detected using the MRM mode by monitoring specific transitions under positive electrospray on API 3200 triple quadrupole LC/MS/MS mass spectrometer (Applied Biosystems/Sciex Instruments). Quantification was done by comparing individual ion peak areas to that of an internal standard. Plasma acylcarnitines were measured on an API 3200 triple quadrupole LC/MS/MS as described (Sunny et al., 2010). Briefly, free carnitine and acylcarnitines were extracted from plasma and then individual acylcarnitine peaks were quantified by comparison with a ^{13}C internal standard (Cambridge Isotopes, Andover, MA). Hepatic ceramides were quantified by LC/MS/MS technology as described (Holland et al., 2011; Tao et al., 2017) using a Shimadzu Nexera X2 UHPLC system coupled to a Shimadzu LCMS-8050 triple quadrupole mass spectrometer operating Ion Source in ESI positive mode. Lipid species were identified based on their molecular mass and fragmentation patterns and verified by lipid standards. Hepatic DAG was quantified as described (Gao et al., 2016; Gao et al., 2017; Simons et al., 2012). Briefly, liver samples were homogenized and extracted with a modified Bligh-Dyer extraction. Samples were infused into a Sciex TripleTOF 6600 mass spectrometer and analyzed using MS/MS^{ALL} analysis with product-ion spectra collected at each unit mass from 200 to 1200 DA. Hepatic cholesterol and triglycerides were measured by an enzymatic assay as described (Zhang et al., 2012).

Hyperinsulinemic-Euglycemic Clamp Studies—On the day of the experiment, food was removed 1 hr after the lights were turned on to start a 4 hr fast. At t = −90 min, a

continuous infusion of HPLC-purified 3-[^{3}H] glucose (0.05 μCi/min) was started to measure glucose turnover. Basal blood samples were collected at t = −15 and −5 min from the tail. At t = 0 min, a single bolus of FGF21 or FGF19 (1 mg/kg) or vehicle alone was i.v. infused. This was followed immediately by continuous infusion of insulin (4 mU/kg/min) together with either FGF19 or FGF21 (16 μg/kg/min) or vehicle alone, with the tracer infusion increased to 0.1 μCi/min. Blood glucose levels were measured every 10 min and a 50% dextrose solution was infused to maintain the blood glucose levels at approximately 150 mg/dl. Steady state occurred at t = 80–120 min. Approximately 15 μl of tail blood was collected at t = 80, 100 and 120 min to determine glucose turnover.

Sympathetic Nerve Activity Measurements—Sympathetic nerve activity (SNA) subserving BAT was measured as described (Morgan and Rahmouni, 2010; Owen et al., 2014). After establishing baseline values, mice were either i.c.v. or i.v. (jugular vein) injected with FGF19 or vehicle (150 mM NaCl, 20 mM Tris and 50% (w/v) glycerol at pH 7.5). SNA was recorded for an additional 4 hr. The volume of all i.c.v. injections was 2 μl.

Cerebrospinal Fluid (CSF) Collection and bFKB1 Measurement—CSF collection was performed as described (Liu and Duff, 2008). Following anesthesia with Avertin (Sigma-Aldrich), the mice were shaved on the back of the neck and placed on a stereotaxic instrument. After swabbing the surgical site with an alcohol prep pad, a dissection microscope was used to expose the dura mater of the cisterna magna. The dura mater was penetrated by a capillary tube and the CSF was collected by osmotic pressure and frozen immediately in liquid nitrogen. bFKB1 concentrations were measured using a human IgG ELISA kit (Affymetrix eBioscience).

Western Blot Analysis—Protein from fresh-frozen liver tissue was extracted using a homogenizer (Fisher Scientific) in 1 x RIPA buffer (Cell Signaling Technology) supplemented with a cocktail of protease and phosphatase inhibitors (Roche). Protein lysate concentrations were measured using the Bradford Protein Assay (Bio-Rad). Equal protein amounts were loaded and electrophoresed in a 4–20% SDS-PAGE gel (Bio-Rad) and transferred to nitrocellulose membranes (Bio-Rad). Membranes were blocked with 5% BSA in Tris-buffered saline with 0.5% Tween-20 (TBST) for 1 hr. Probing of membranes with antibodies against p-ERK1/2 and T-ERK1/2 (Cell Signaling Technology) was performed overnight at 4°C. Membranes were then incubated with secondary antibody for 1 hr at room temperature. Membranes were developed using the Pierce ECL Western Blotting Substrate (Thermo Fisher Scientific) and signal was detected with an ImageQuant LAS4000 luminescent imager (General Electric). Quantification was done using ImageJ.

Real-time Quantitative PCR Analyses—Total RNA from liver and BAT was extracted by Stat 60 reagent (IsoTex Diagnostics, Inc.).

Total RNA from WAT was extracted by RNeasy lipid tissue mini kits (Qiagen). cDNA was synthesized from 2 μg of RNA (Invitrogen). QPCR was performed using SYBR GreenER as described (Bookout et al., 2006). Primers are listed in Table S1.

QUANTIFICATION AND STATISTICAL ANALYSIS

Mean values ± SEM are shown. Two-way ANOVA with Holm-Sidak post hoc correction (GraphPad Prism) was used for multiple group analyses. Student's t test (GraphPad Prism) was used for two-group analyses. Differences were considered statistically significant at $p < 0.05$.

Supplementary Material

Refer to Web version on PubMed Central for supplementary material.

Acknowledgments

We thank Kelly Suino-Powell and Eric Xu (Van Andel Institute) for providing recombinant FGF19 and Birgitte Anderson and Novo Nordisk for providing recombinant FGF21. We thank Hamid Mirzaei for FGF15 measurements; Ruth Gordillo, Duyen Do and Eva Mason in the UT Southwestern Metabolic Phenotyping Core for ceramide measurements; Jeffrey McDonald for diacylglycerol measurements; David Chen, Ankit Sharma and Zeke Quittner-Strom for assistance with mouse clamp experiments; and Yuan Zhang, Heather Lawrence, Ewa Borowicz and Kevin Vale for technical assistance. This work was supported by the National Institutes of Health (R01DK067158 to S.A.K. and D.J.M.); the Robert A. Welch Foundation (grants I-1804 to S.C.B., I-1558 to S.A.K. and I-1275 to D.J.M.); and the Howard Hughes Medical Institute (D.J.M.).

References

Adams AC, Yang C, Coskun T, Cheng CC, Gimeno RE, Luo Y, Kharitonenkov A. The breadth of FGF21's metabolic actions are governed by FGFR1 in adipose tissue. Molecular metabolism. 2012; 2:31–37. [PubMed: 24024127]

BonDurant LD, Ameka M, Naber MC, Markan KR, Idiga SO, Acevedo MR, Walsh SA, Ornitz DM, Potthoff MJ. FGF21 Regulates Metabolism Through Adipose-Dependent and -Independent Mechanisms. Cell Metab. 2017; 25:935–944. e934. [PubMed: 28380381]

Bookout AL, Cummins CL, Mangelsdorf DJ, Pesola JM, Kramer MF. High-throughput real-time quantitative reverse transcription PCR. Curr Protoc Mol Biol. 2006; Chapter 15(Unit 15.18)

Bookout AL, de Groot MH, Owen BM, Lee S, Gautron L, Lawrence HL, Ding X, Elmquist JK, Takahashi JS, Mangelsdorf DJ, Kliewer SA. FGF21 regulates metabolism and circadian behavior by acting on the nervous system. Nature Med. 2013; 19:1147–1152. [PubMed: 23933984]

Casetta B, Tagliacozzi D, Shushan B, Federici G. Development of a method for rapid quantitation of amino acids by liquid chromatography-tandem mass spectrometry (LC-MSMS) in plasma. Clinical chemistry and laboratory medicine. 2000; 38:391–401. [PubMed: 10952221]

Choi M, Moschetta A, Bookout AL, Peng L, Umetani M, Holmstrom SR, Suino-Powell K, Xu HE, Richardson JA, Gerard RD, Mangelsdorf DJ, Kliewer SA. Identification of a hormonal basis for gallbladder filling. Nat Med. 2006; 12:1253–1255. [PubMed: 17072310]

Coskun T, Bina HA, Schneider MA, Dunbar JD, Hu CC, Chen Y, Moller DE, Kharitonenkov A. Fibroblast growth factor 21 corrects obesity in mice. Endocrinology. 2008; 149:6018–6027. [PubMed: 18687777]

Ding X, Boney-Montoya J, Owen BM, Bookout AL, Coate KC, Mangelsdorf DJ, Kliewer SA. betaKlotho is required for fibroblast growth factor 21 effects on growth and metabolism. Cell Metab. 2012; 16:387–393. [PubMed: 22958921]

Douris N, Stevanovic D, Fisher FM, Cisu TI, Chee MJ, Ly Nguyen N, Zarebidaki E, Adams AC, Kharitonenkov A, Flier JS, Bartness TJ, Maratos-Flier E. Central Fibroblast Growth Factor 21 Browns White Fat via Sympathetic Action in Male Mice. Endocrinology. 2015:en20142001.

Fisher FM, Estall JL, Adams AC, Antonellis PJ, Bina HA, Flier JS, Kharitonenkov A, Spiegelman BM, Maratos-Flier E. Integrated regulation of hepatic metabolism by fibroblast growth factor 21 (FGF21) in vivo. Endocrinology. 2011; 152:2996–3004. [PubMed: 21712364]

Fisher FM, Kleiner S, Douris N, Fox EC, Mepani RJ, Verdeguer F, Wu J, Kharitonenkov A, Flier JS, Maratos-Flier E, Spiegelman BM. FGF21 regulates PGC-1alpha and browning of white adipose tissues in adaptive thermogenesis. Genes Dev. 2012; 26:271–281. [PubMed: 22302939]

Fisher FM, Maratos-Flier E. Understanding the Physiology of FGF21. Annu Rev Physiol. 2016; 78:223–241. [PubMed: 26654352]

Foltz IN, Hu S, King C, Wu X, Yang C, Wang W, Weiszmann J, Stevens J, Chen JS, Nuanmanee N, Gupte J, Komorowski R, Sekirov L, Hager T, Arora T, Ge H, Baribault H, Wang F, Sheng J, Karow M, Wang M, Luo Y, McKeehan W, Wang Z, Véniant MM, Li Y. Treating Diabetes and Obesity with an FGF21-Mimetic Antibody Activating the βKlotho/FGFR1c Receptor Complex. Sci Transl Med. 2012; 4:162ra153–162ra153.

Fon Tacer K, Bookout AL, Ding X, Kurosu H, John GB, Wang L, Goetz R, Mohammadi M, Kuro-o M, Mangelsdorf DJ, Kliewer SA. Research resource: Comprehensive expression atlas of the fibroblast growth factor system in adult mouse. Mol Endocrinol. 2010; 24:2050–2064. [PubMed: 20667984]

Fu L, John LM, Adams SH, Yu XX, Tomlinson E, Renz M, Williams PM, Soriano R, Corpuz R, Moffat B, Vandlen R, Simmons L, Foster J, Stephan JP, Tsai SP, Stewart TA. Fibroblast growth factor 19 increases metabolic rate and reverses dietary and leptin-deficient diabetes. Endocrinology. 2004; 145:2594–2603. [PubMed: 14976145]

Gao F, McDaniel J, Chen EY, Rockwell H, Lynes MD, Tseng YH, Sarangarajan R, Narain NR, Kiebish MA. Monoacylglycerol Analysis Using MS/MS(ALL) Quadruple Time of Flight Mass Spectrometry. Metabolites. 2016; 6

Gao F, McDaniel J, Chen EY, Rockwell HE, Drolet J, Vishnudas VK, Tolstikov V, Sarangarajan R, Narain NR, Kiebish MA. Dynamic and temporal assessment of human dried blood spot MS/MSALL shotgun lipidomics analysis. Nutr Metab (Lond). 2017; 14:28. [PubMed: 28344632]

Holland WL, Adams AC, Brozinick JT, Bui HH, Miyauchi Y, Kusminski CM, Bauer SM, Wade M, Singhal E, Cheng CC, Volk K, Kuo MS, Gordillo R, Kharitonenkov A, Scherer PE. An FGF21-adiponectin-ceramide axis controls energy expenditure and insulin action in mice. Cell Metab. 2013; 17:790–797. [PubMed: 23663742]

Holland WL, Miller RA, Wang ZV, Sun K, Barth BM, Bui HH, Davis KE, Bikman BT, Halberg N, Rutkowski JM, Wade MR, Tenorio VM, Kuo MS, Brozinick JT, Zhang BB, Birnbaum MJ, Summers SA, Scherer PE. Receptor-mediated activation of ceramidase activity initiates the pleiotropic actions of adiponectin. Nat Med. 2011; 17:55–63. [PubMed: 21186369]

Hondares E, Rosell M, Gonzalez FJ, Giralt M, Iglesias R, Villarroya F. Hepatic FGF21 expression is induced at birth via PPARalpha in response to milk intake and contributes to thermogenic activation of neonatal brown fat. Cell Metab. 2010; 11:206–212. [PubMed: 20197053]

Hsuchou H, Pan W, Kastin AJ. The fasting polypeptide FGF21 can enter brain from blood. Peptides. 2007; 28:2382–2386. [PubMed: 17996984]

Hsuchou H, Pan W, Kastin AJ. Fibroblast growth factor 19 entry into brain. Fluids Barriers CNS. 2013; 10:32. [PubMed: 24176017]

Ito S, Fujimori T, Furuya A, Satoh J, Nabeshima Y. Impaired negative feedback suppression of bile acid synthesis in mice lacking betaKlotho. J Clin Invest. 2005; 115:2202–2208. [PubMed: 16075061]

Katafuchi T, Esterhazy D, Lemoff A, Ding X, Sondhi V, Kliewer SA, Mirzaei H, Mangelsdorf DJ. Detection of FGF15 in plasma by stable isotope standards and capture by anti-peptide antibodies and targeted mass spectrometry. Cell Metab. 2015; 21:898–904. [PubMed: 26039452]

Kharitonenkov A, Adams AC. Inventing new medicines: The FGF21 story. Mol Metab. 2014; 3:221–229. [PubMed: 24749049]

Kharitonenkov A, DiMarchi R. Fibroblast growth factor 21 night watch: advances and uncertainties in the field. J Intern Med. 2017; 281:233–246. [PubMed: 27878865]

Kharitonenkov A, Shiyanova TL, Koester A, Ford AM, Micanovic R, Galbreath EJ, Sandusky GE, Hammond LJ, Moyers JS, Owens RA, Gromada J, Brozinick JT, Hawkins ED, Wroblewski VJ, Li DS, Mehrbod F, Jaskunas SR, Shanafelt AB. FGF-21 as a novel metabolic regulator. J Clin Invest. 2005; 115:1627–1635. [PubMed: 15902306]

Kir S, Beddow SA, Samuel VT, Miller P, Previs SF, Suino-Powell K, Xu HE, Shulman GI, Kliewer SA, Mangelsdorf DJ. FGF19 as a postprandial, insulin-independent activator of hepatic protein and glycogen synthesis. Science. 2011; 331:1621–1624. [PubMed: 21436455]

Kolumam G, Chen MZ, Tong R, Zavala-Solorio J, Kates L, van Bruggen N, Ross J, Wyatt SK, Gandham VD, Carano RA, Dunshee DR, Wu AL, Haley B, Anderson K, Warming S, Rairdan XY, Lewin-Koh N, Zhang Y, Gutierrez J, Baruch A, Gelzleichter TR, Stevens D, Rajan S, Bainbridge TW, Vernes JM, Meng YG, Ziai J, Soriano RH, Brauer MJ, Chen Y, Stawicki S, Kim HS, Comps-Agrar L, Luis E, Spiess C, Wu Y, Ernst JA, McGuinness OP, Peterson AS, Sonoda J. Sustained Brown Fat Stimulation and Insulin Sensitization by a Humanized Bispecific Antibody Agonist for Fibroblast Growth Factor Receptor 1/betaKlotho Complex. EBioMedicine. 2015; 2:730–743. [PubMed: 26288846]

Kuro-o M. Klotho and betaKlotho. Adv Exp Med Biol. 2012; 728:25–40. [PubMed: 22396160]

Lin Z, Tian H, Lam KS, Lin S, Hoo RC, Konishi M, Itoh N, Wang Y, Bornstein SR, Xu A, Li X. Adiponectin mediates the metabolic effects of FGF21 on glucose homeostasis and insulin sensitivity in mice. Cell Metab. 2013; 17:779–789. [PubMed: 23663741]

Liu L, Duff K. A Technique for Serial Collection of Cerebrospinal Fluid from the Cisterna Magna in Mouse. J Vis Exp. 2008:960. [PubMed: 19066529]

Marcelin G, Jo YH, Li X, Schwartz GJ, Zhang Y, Dun NJ, Lyu RM, Blouet C, Chang JK, Chua S Jr. Central action of FGF19 reduces hypothalamic AGRP/NPY neuron activity and improves glucose metabolism. Molecular metabolism. 2014; 3:19–28. [PubMed: 24567901]

Markan KR, Naber MC, Ameka MK, Anderegg MD, Mangelsdorf DJ, Kliewer SA, Mohammadi M, Potthoff MJ. Circulating FGF21 is Liver Derived and Enhances Glucose Uptake During Refeeding and Overfeeding. Diabetes. 2014

Martens K, Bottelbergs A, Baes M. Ectopic recombination in the central and peripheral nervous system by aP2/FABP4-Cre mice: implications for metabolism research. FEBS letters. 2010; 584:1054–1058. [PubMed: 20138876]

Morgan DA, Rahmouni K. Differential effects of insulin on sympathetic nerve activity in agouti obese mice. J Hypertens. 2010; 28:1913–1919. [PubMed: 20577122]

Morton GJ, Matsen ME, Bracy DP, Meek TH, Nguyen HT, Stefanovski D, Bergman RN, Wasserman DH, Schwartz MW. FGF19 action in the brain induces insulin-independent glucose lowering. J Clin Invest. 2013; 123:4799–4808. [PubMed: 24084738]

Owen BM, Ding X, Morgan DA, Coate KC, Bookout AL, Rahmouni K, Kliewer SA, Mangelsdorf DJ. FGF21 acts centrally to induce sympathetic nerve activity, energy expenditure, and weight loss. Cell Metab. 2014; 20:670–677. [PubMed: 25130400]

Owen BM, Mangelsdorf DJ, Kliewer SA. Tissue-specific actions of the metabolic hormones FGF15/19 and FGF21. Trends in endocrinology and metabolism: TEM. 2015; 26:22–29. [PubMed: 25476453]

Perry RJ, Lee S, Ma L, Zhang D, Schlessinger J, Shulman GI. FGF1 and FGF19 reverse diabetes by suppression of the hypothalamic-pituitary-adrenal axis. Nat Commun. 2015; 6:6980. [PubMed: 25916467]

Ryan KK, Kohli R, Gutierrez-Aguilar R, Gaitonde SG, Woods SC, Seeley RJ. Fibroblast growth factor-19 action in the brain reduces food intake and body weight and improves glucose tolerance in male rats. Endocrinology. 2013; 154:9–15. [PubMed: 23183168]

Sarruf DA, Thaler JP, Morton GJ, German J, Fischer JD, Ogimoto K, Schwartz MW. Fibroblast growth factor 21 action in the brain increases energy expenditure and insulin sensitivity in obese rats. Diabetes. 2010; 59:1817–1824. [PubMed: 20357365]

Simons B, Kauhanen D, Sylvanne T, Tarasov K, Duchoslav E, Ekroos K. Shotgun Lipidomics by Sequential Precursor Ion Fragmentation on a Hybrid Quadrupole Time-of-Flight Mass Spectrometer. Metabolites. 2012; 2:195–213. [PubMed: 24957374]

Sunny NE, Satapati S, Fu X, He T, Mehdibeigi R, Spring-Robinson C, Duarte J, Potthoff MJ, Browning JD, Burgess SC. Progressive adaptation of hepatic ketogenesis in mice fed a high-fat diet. Am J Physiol Endocrinol Metab. 2010; 298:E1226–1235. [PubMed: 20233938]

Tabrizi M, Bornstein GG, Suria H. Biodistribution mechanisms of therapeutic monoclonal antibodies in health and disease. The AAPS journal. 2010; 12:33–43. [PubMed: 19924542]

Tao C, Holland WL, Wang QA, Shao M, Jia L, Sun K, Lin X, Kuo YC, Johnson JA, Gordillo R, Elmquist JK, Scherer PE. Short-Term vs. Long-Term Effects of Adipocyte Toll-like Receptor 4 Activation on Insulin Resistance in Male Mice. Endocrinology. 2017

Tomlinson E, Fu L, John L, Hultgren B, Huang X, Renz M, Stephan JP, Tsai SP, Powell-Braxton L, French D, Stewart TA. Transgenic mice expressing human fibroblast growth factor-19 display increased metabolic rate and decreased adiposity. Endocrinology. 2002; 143:1741–1747. [PubMed: 11956156]

Wu AL, Coulter S, Liddle C, Wong A, Eastham-Anderson J, French DM, Peterson AS, Sonoda J. FGF19 regulates cell proliferation, glucose and bile acid metabolism via FGFR4-dependent and independent pathways. PLoS One. 2011a; 6:e17868. [PubMed: 21437243]

Wu AL, Kolumam G, Stawicki S, Chen Y, Li J, Zavala-Solorio J, Phamluong K, Feng B, Li L, Marsters S, Kates L, van Bruggen N, Leabman M, Wong A, West D, Stern H, Luis E, Kim HS, Yansura D, Peterson AS, Filvaroff E, Wu Y, Sonoda J. Amelioration of type 2 diabetes by antibody-mediated activation of fibroblast growth factor receptor 1. Sci Transl Med. 2011b; 3:113ra126.

Xu J, Lloyd DJ, Hale C, Stanislaus S, Chen M, Sivits G, Vonderfecht S, Hecht R, Li YS, Lindberg RA, Chen JL, Jung DY, Zhang Z, Ko HJ, Kim JK, Veniant MM. Fibroblast growth factor 21 reverses hepatic steatosis, increases energy expenditure, and improves insulin sensitivity in diet-induced obese mice. Diabetes. 2009; 58:250–259. [PubMed: 18840786]

Yu C, Wang F, Kan M, Jin C, Jones RB, Weinstein M, Deng CX, McKeehan WL. Elevated cholesterol metabolism and bile acid synthesis in mice lacking membrane tyrosine kinase receptor FGFR4. J Biol Chem. 2000; 275:15482–15489. [PubMed: 10809780]

Zhang J, Gupte J, Gong Y, Weiszmann J, Zhang Y, Lee KJ, Richards WG, Li Y. Chronic Over-expression of Fibroblast Growth Factor 21 Increases Bile Acid Biosynthesis by Opposing FGF15/19 Action. EBioMedicine. 2017; 15:173–183. [PubMed: 28041926]

Zhang Y, Xie Y, Berglund ED, Coate KC, He TT, Katafuchi T, Xiao G, Potthoff MJ, Wei W, Wan Y, Yu RT, Evans RM, Kliewer SA, Mangelsdorf DJ. The starvation hormone, fibroblast growth factor-21, extends lifespan in mice. Elife. 2012; 1:e00065. [PubMed: 23066506]

Highlights

- FGF19 and FGF21 act through a common tissue-specific mechanism to cause weight loss
- The nervous system is the direct target for FGF19 and FGF21 effects on weight loss
- β–Klotho in adipose and liver is dispensable for FGF19/FGF21 effects on weight loss
- An FGF21 mimetic antibody mediates its weigh loss effects via the nervous system

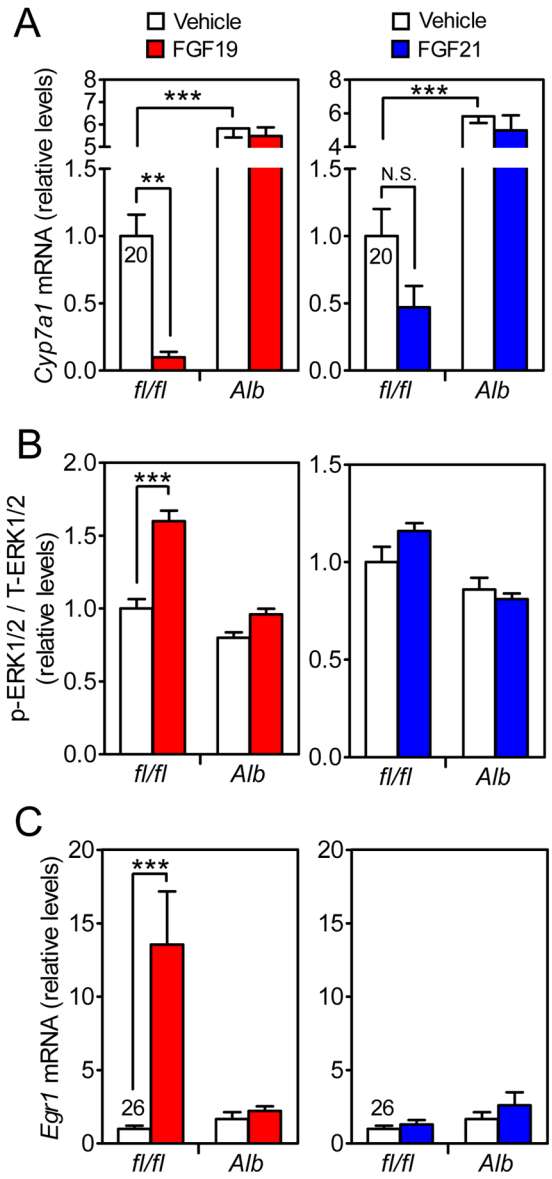

Figure 1. FGF19 but not FGF21 has robust direct effects on hepatocytes under acute treatment conditions

(A) DIO *Klb*$^{fl/fl}$ and *Klb*^{Alb} littermates were i.p. injected with 1 mg/kg FGF19, FGF21 or vehicle and sacrificed 6 hr later. *Cyp7a1* mRNA in liver was measured by QPCR. n = 5/group.

(B and C) DIO *Klb*$^{fl/fl}$ and *Klb*^{Alb} littermates were i.p. injected with 1 mg/kg FGF19, FGF21 or vehicle and sacrificed 30 min later. (B) Phosphorylated ERK1/2 normalized to total ERK1/2 protein in liver was measured by western blot. (C) *Egr1* mRNA levels in liver was measured by QPCR. n = 6/group. QPCR cycle time values are shown for the vehicle-treated *Klb*$^{fl/fl}$ group.

Data are shown as the mean ± SEM. **p < 0.01, ***p<0.001 compared to control. N.S., not significant. Significant interactions between genotype (*Klb*$^{fl/fl}$ vs. *Klb*^{Alb}) and treatment

(Vehicle vs. FGF19) were detected for p-ERK1/2/T-ERK/1/2 (p=0.0007) and *Egr1* mRNA (p=0.004).

See also Figure S1 and Table S1.

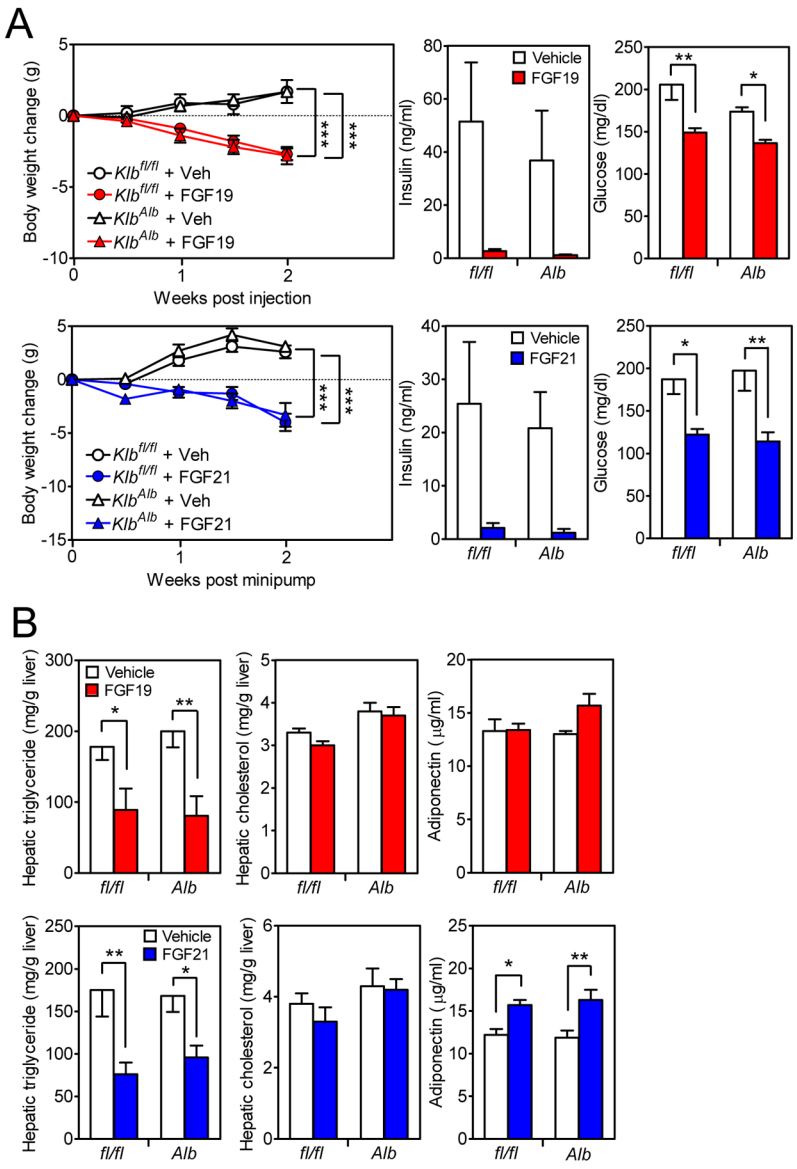

Figure 2. β-Klotho in liver is not required for FGF19 and FGF21 to cause weight loss

(A and B) DIO $Klb^{fl/fl}$ and Klb^{Alb} littermates were treated with FGF19, FGF21 or vehicle for 2 wk. (A) Body weight change, plasma insulin and glucose levels and (B) hepatic triglyceride and cholesterol levels and plasma adiponectin levels were measured. n = 5–6/group.

Data are shown as the mean ± SEM. *p < 0.05, **p < 0.01, ***p<0.001 compared to control.

See also Figures S1 and S2, and Table S1.

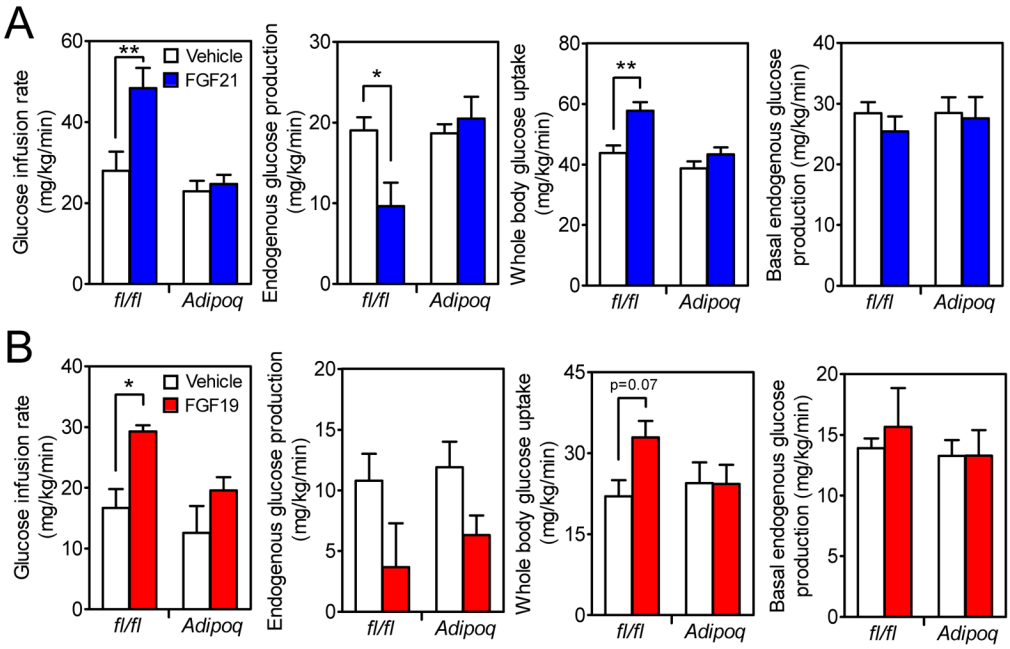

Figure 3. β-Klotho in adipose tissue is required for the acute insulin-sensitizing actions of FGF21 and FGF19

(A) DIO $Klb^{fl/fl}$ and Klb^{Adipoq} littermates were treated with FGF21 or vehicle during a hyperinsulinemic-euglycemic clamp and glucose infusion rate, endogenous glucose production and whole-body glucose uptake during the clamp and basal endogenous glucose production measured. n = 5–6/group.

(B) DIO $Klb^{fl/fl}$ and Klb^{Adipoq} littermates were treated with FGF19 or vehicle during a hyperinsulinemic-euglycemic clamp and glucose infusion rate, endogenous glucose production and whole-body glucose uptake during the clamp and basal endogenous glucose production measured. n = 6–8/group.

Data are shown as the mean ± SEM. *p < 0.05, **p < 0.01 compared to control. Significant interactions between genotype ($Klb^{fl/fl}$ vs. Klb^{Adipoq}) and treatment (Vehicle vs. FGF21) were detected for glucose infusion rate (p=0.03) and endogenous glucose production (p=0.02).

See also Table S1.

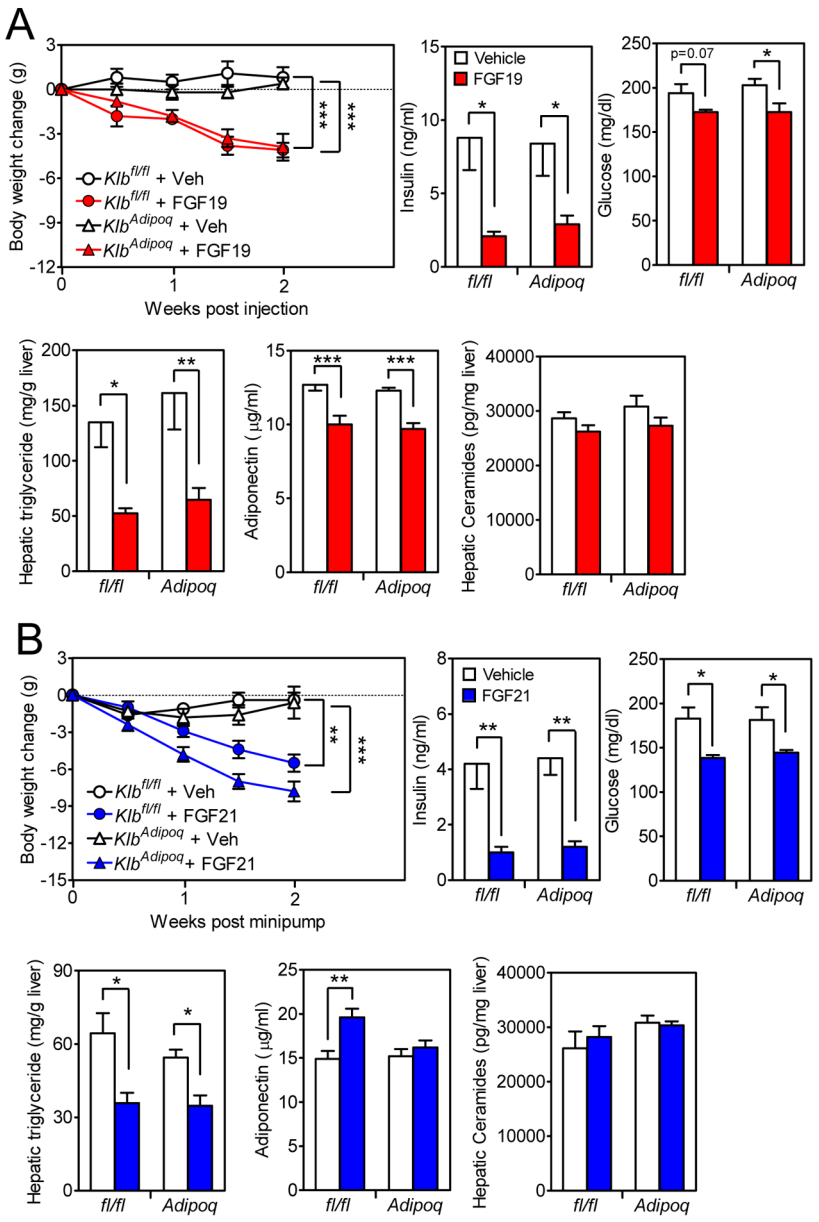

Figure 4. β-Klotho in adipose tissue is not required for FGF19 and FGF21 to cause weight loss

(A and B) DIO *Klb*$^{fl/fl}$ and *Klb*^{Adipoq} littermates were treated with FGF19, FGF21 or vehicle for 2 wk. Body weight change, plasma insulin and glucose levels, hepatic triglyceride levels, plasma adiponectin levels and hepatic ceramide concentrations were measured. n = 5–6/ group.

Data are shown as the mean ± SEM. *p < 0.05, **p < 0.01, ***p<0.001 compared to control.

See also Figure S1 and S3, and Table S1.

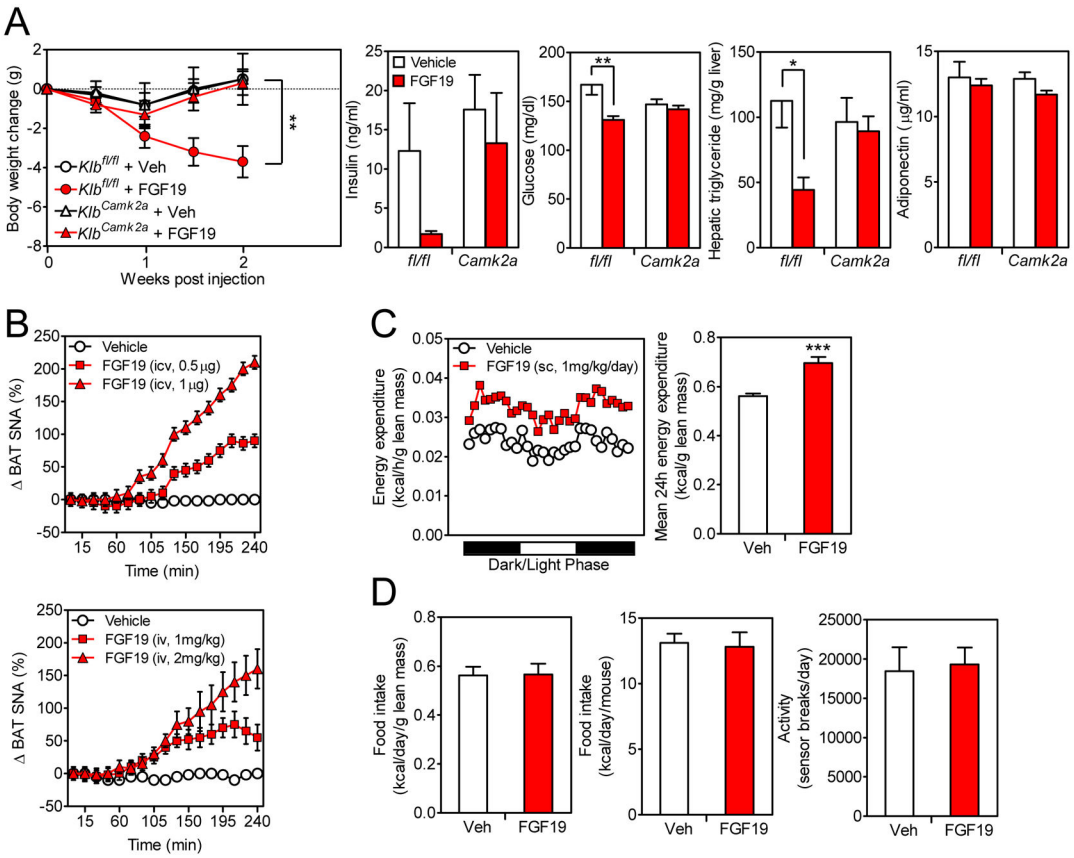

Figure 5. FGF19 acts on the nervous system to cause weight loss

(A) DIO *Klb*$^{fl/fl}$ and *Klb*^{Camk2a} littermates were administered FGF19 or vehicle for 2 wk. Body weight, plasma insulin and glucose levels, hepatic triglyceride levels and plasma adiponectin levels were measured. n = 5–6/group.

(B) Percent change in sympathetic nerve activity subserving BAT was recorded in mice following i.c.v. (top panel) or i.v. (bottom panel) injection of FGF19 at the indicated doses or vehicle. n = 7–8/group.

(C) Representative 24 hr energy expenditure in DIO mice administered FGF19 or vehicle (left panel). Quantification of 24 hr energy expenditure for the same mice (right panel). n = 5/group.

(D) 24 hr food intake (left and middle panels) and activity (right panel) in DIO mice treated with FGF19 or vehicle as in (C). n = 5/group.

Data are shown as the mean ± SEM. *p < 0.05, **p < 0.01, ***p<0.001 compared to control. Significant interactions between genotype (*Klb*$^{fl/fl}$ vs. *Klb*^{Camk2a}) and treatment (Vehicle vs. FGF19) were detected for body weight change at week 2 (p=0.04) and plasma glucose (p=0.02).

See also Figure S1 and S4, and Table S1.

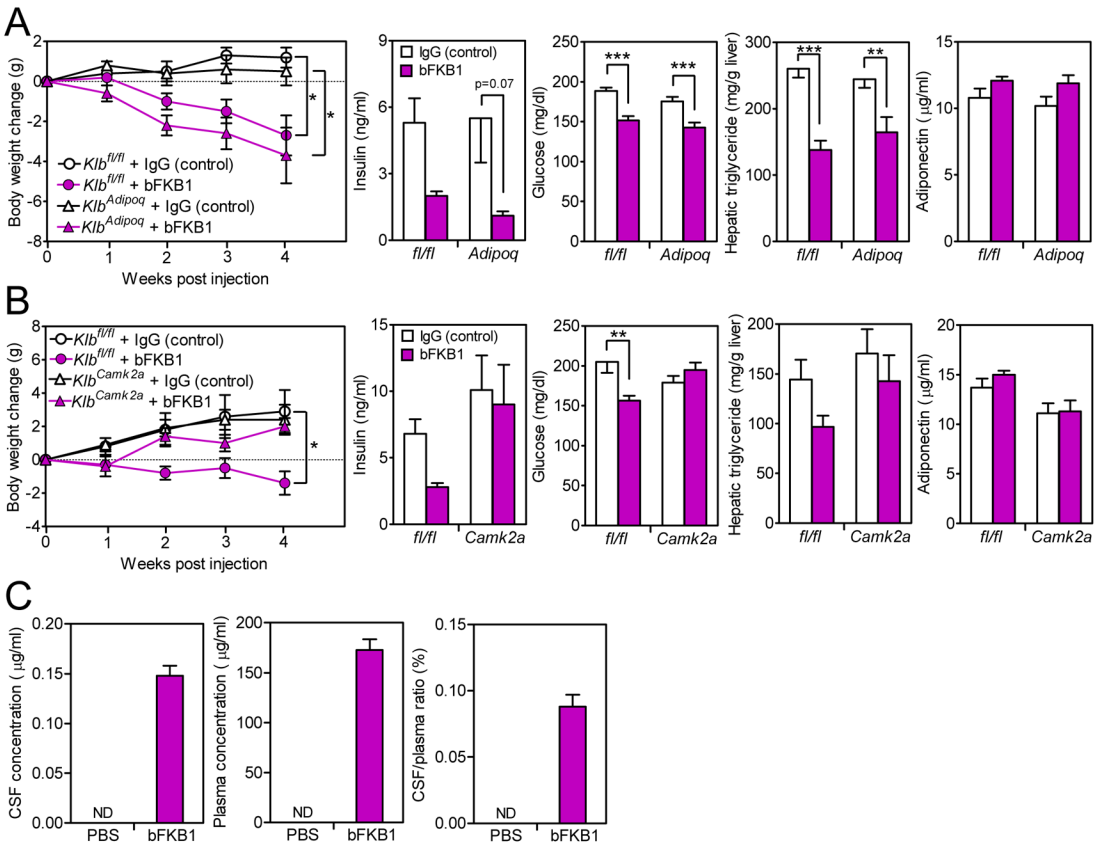

Figure 6. The FGFR1c/β-Klotho activating antibody acts directly on the nervous system to regulate body weight and circulating glucose and insulin levels

(A) DIO *Klb*$^{fl/fl}$ and *Klb*^{Adipoq} littermates were administered either bFKB1 or control antibody (trastuzumab) for 4 wk, with dosing every two weeks. Body weight change, plasma insulin and glucose levels, hepatic triglyceride levels and plasma adiponectin levels were measured. n = 6/group.

(B) DIO *Klb*$^{fl/fl}$ and *Klb*^{Camk2a} littermates were administered bFKB1 or control antibody (trastuzumab) for 4 wk. Body weight change, plasma insulin and glucose levels, hepatic triglyceride levels and plasma adiponectin levels were measured. n = 6/group.

(C) bFKB1 levels in the cerebrospinal fluid (CSF) and plasma were measured in DIO mice 10 days after i.p. injection of bFKB1 or PBS (left and middle panels). CSF/plasma ratio for bFKB1 (right panel). n = 4–5/group.

Data are shown as the mean ± SEM. *p < 0.05, **p < 0.01, ***p<0.001 compared to control. ND, not detected. Significant interactions between genotype (*Klb*$^{fl/fl}$ vs. *Klb*^{Camk2a}) and treatment (control IgG vs. bFKB1) were detected for body weight change at week 4 (p=0.04) and plasma glucose (p=0.004).

See also Figure S5 and Table S1.